

# Effects of different thermoplastic binders on the processability of feedstocks for ceramic co-extrusion process

M.R. Ismael<sup>a,b,\*</sup>, F. Clemens<sup>a</sup>, T. Graule<sup>a</sup>, M.J. Hoffmann<sup>b</sup>

<sup>a</sup> *Laboratory for High Performance Ceramics, Swiss Federal Laboratories for Materials Testing and Research, Ueberlandstrasse 129, 8600 Duebendorf, Switzerland*

<sup>b</sup> *Karlsruhe Institute of Technology, Institute of Ceramics in Mechanical Engineering, Heid-und-Neustr. 7, 76131 Karlsruhe, Germany*

Received 17 January 2011; received in revised form 15 May 2011; accepted 18 May 2011

Available online 26 May 2011

## Abstract

The co-extrusion process involves the simultaneous extrusion of multiple materials, such as ceramic–thermoplastic feedstocks that can be used to manufacture fine-scaled piezocomposites, for both structural and functional applications. The primary step in the development of the feedstocks is the selection of the optimal thermoplastic binder with the function of providing plasticity as well as proper rheological behavior to the ceramic material during processing. The objective of the present work was to investigate the effects of different commercially available thermoplastic binders (polystyrene, low-density polyethylene, poly(ethylene-co-ethyl acrylate) and a blend of poly(ethylene-co-ethyl acrylate) and poly(isobutyl methacrylate)) on the processability of highly loaded lead zirconate titanate (PZT) feedstocks, suitable for the co-extrusion process. After characterizing the thermal behavior of the binders by means of TG and DSC analyses, the flow behavior of the unfilled polymers was analyzed and compared with the corresponding PZT-filled mixture (58 vol.% PZT) applying torque rheometry. Using an Arrhenius relation, the temperature dependency of viscosity was determined and the energy of activation for the viscous flow calculated. Due to the fact that the polyethylene presented a low viscosity with a high solid loading, no indication of degradation, a strong polymer–particle interaction as well as a comparatively low die swell, this thermoplastic binder was used in the formulation of PZT feedstocks to successfully produce thin solid (240  $\mu\text{m}$  diameter) and hollow (800  $\mu\text{m}$  diameter) PZT fibers by the co-extrusion technique.

© 2011 Elsevier Ltd and Techna Group S.r.l. All rights reserved.

**Keywords:** A. Extrusion; D. PZT; Fibers; Rheology

## 1. Introduction

The principle of the ceramic co-extrusion technique consists of assembling a macro-scaled preform composite and afterwards extruding it using an appropriate barrel and die [1,2]. Assembling the first extruded structures the process can be repeated until that the desired scale is achieved, limited by the particle size of the starting powder. Alternatively, a complex die in which multiple materials flow together into the desired structure can be used for the reduction [3]. The co-extrusion method is dependent on the flow properties of the different materials. To achieve co-extruded composites identical in their

geometry and composition to the original preform, albeit with reduced cross-sectional dimensions, tailoring the rheology of the different materials being co-extruded is essential in preventing flow-related failures [2]. The ceramic co-extrusion technology has been proven to be effective to fabricate fibrous monolithic composites [4], multi-material multifunctional fibers [5], spiral-shaped piezoelectric actuators [6] as well as helical-shaped piezoelectric ultrasonic motors [7].

The whole process chain includes the following steps: (a) feedstocks compounding, which involves the mixing of a ceramic powder with an organic vehicle, (b) preform fabrication and co-extrusion, (c) removal of the organic vehicle (debinding) and, finally, (d) sintering of the body to near full density [1,2]. The first requirement for the high-performance ceramic co-extrusion process, as well as the extrusion and injection molding techniques, is to attain a feedstock with the desired plasticity. To accomplish this condition, the organic vehicle often used is a thermoplastic binder [1,2,4,6–10]. In addition to provide the

\* Corresponding author at: Laboratory for High Performance Ceramics, Swiss Federal Laboratories for Materials Testing and Research, Ueberlandstrasse 129, 8600 Duebendorf, Switzerland. Tel.: +41 44 823 41 06; fax: +41 44 823 41 50.

E-mail address: [marina.rojas.ismael@gmail.com](mailto:marina.rojas.ismael@gmail.com) (M.R. Ismael).

plasticity and modify the rheological behavior of the ceramic feedstock, the thermoplastic binders confer handling strength and perform as a backbone material to the as-shaped ceramic bodies. Their presence, however, creates significant challenges, especially for components such as filaments and thin structures. The binder must show thermal stability under mixing and shaping conditions because binder degradation can drastically change the flow behavior of the feedstocks and therefore influence the geometrical properties of the final product. For practical reasons, it must exhibit high flexibility and a relatively low melt viscosity, particularly when mixed with high solid loading of ceramic powders (50–65 vol.%).

However, not only the viscous part of the composition will be relevant for the co-extrusion process. The elastic forces performing on the materials during co-extrusion also have a significant effect. For example, a common viscoelastic effect is the die swell (or extrudate swell) [11], which happens due to a partial recovery of the elastic deformation that a viscoelastic fluid undergoes during flow through a capillary [12]. Moreover, the thermoplastic binder must confer adequate strength to the body during the initial stage of binder removal and thermally decompose at a relatively low temperature in order not to affect the densification of the ceramic. After shaping, the binder must be removed before the sintering of the ceramic takes place, which is often complex and time consuming. For example, carbon residue from the organic species or uncontrolled decomposition reactions may generate defects like cracks or may entrap air and/or CO<sub>2</sub> during binder removal [13].

Considering the aforementioned challenges, the first step in the development of the thermoplastic co-extrusion process is the selection of the optimal organic binder additives. However, some pre-requisites must be taken into account before the selection. An extensive literature on polymers as binders for ceramics is available [8,13–16], although most of it concerns the binder removal from the green body. As discussed, the foremost criterion for binder selection is that it should provide suitable rheological properties to the ceramic feedstock during processing. How do the polymer properties such as transition temperatures affect the processing behavior of the feedstocks to be co-extruded? How do the interactions between the thermoplastic binders and the ceramic particles affect the processability of the feedstocks? The influence of the binder in the processability of the feedstocks might be predicted by a

systematic characterization of the thermoplastic binders and their corresponding filled system. The objective of the present study is to discuss the effects of different thermoplastic binder characteristics on the processing behavior of lead zirconate titanate (Pb(Zr<sub>x</sub>Ti<sub>1-x</sub>)O<sub>3</sub>; PZT) feedstocks prepared for the co-extrusion process. The motivation for studying PZT-based feedstocks is the increased use of this ferroelectric material in the fiber form to manufacture smart ceramic–polymer composites [17,18]. With the use of the co-extrusion process, PZT fibers with diameter down to 20 μm might be achieved without increasing the extrusion pressure dramatically [2]. PZT thin fibers are desired for such smart composites as they can be operated with increased actuation and magnification.

## 2. Experimental

### 2.1. Selection of the thermoplastic binders to be investigated

There are a large number of polymers that could be used for the thermoplastic shaping process of ceramics. The binders selected to be investigated within this study (Fig. 1) have been extensively used in the thermoplastic extrusion field. Additionally, those binders are commercially available at an adequate price. Polystyrene (PS) has been applied as the organic vehicle for the preparation of extruded zirconia plates [19]. Low density polyethylene (LDPE), a polyolefin containing a highly branched chain structure [11], has been successfully used for the extrusion of polycrystalline ceramic fibers, such as PZT, silicon carbide, and lanthanum strontium manganate [9,10,20]. The poly(ethylene-co-ethyl acrylate) (EEA) copolymer has been mixed with conductive fillers to form electrically conductive polymer composites [21]. The poly(isobutyl methacrylate) (PiBMA) resin was selected with the function to blend the EEA binder. The reason for blending the EEA is based on the fact that its high flexibility can be modified by incorporating a brittle thermoplastic polymer [22]. This blended system has been commonly used for the thermoplastic processing of ceramics by co-extrusion [6,7].

It is worthwhile to mention that several previous investigations with hydrophilic thermoplastics, such as polyamide (PA) and polymethylmethacrylate (PMMA), showed that those materials are not useful for our compounding process, as they

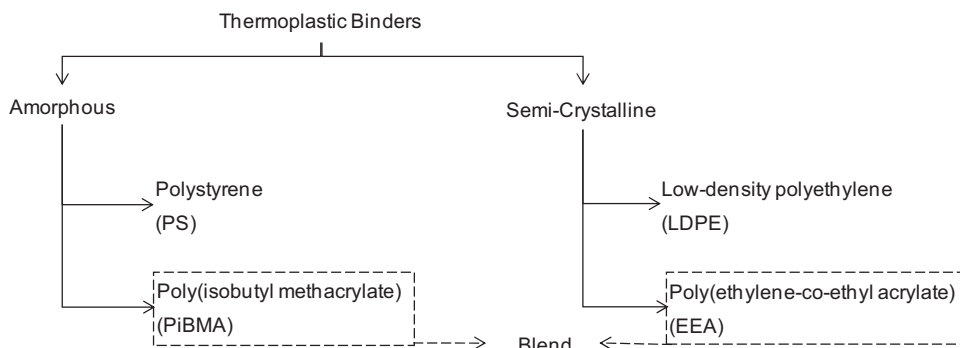


Fig. 1. Thermoplastic binders investigated in this study.

decompose under shear and heat around 10 °C above their melting temperatures. Due to this effect, the property comparison between the unfilled and the ceramic-filled polymers would not be feasible after introducing shear and temperature during compounding. Therefore, only the four aforementioned thermoplastic binders were investigated within this study.

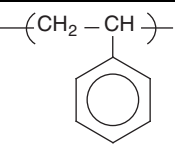
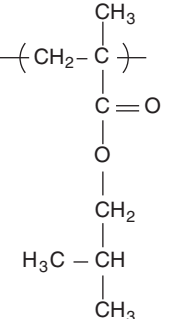
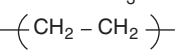
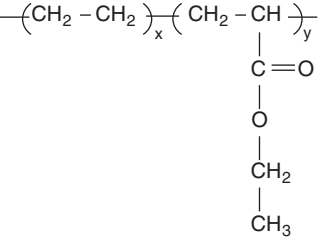
## 2.2. Materials and methods

Table 1 gives further information on all of the polymers studied within this work. The density values were obtained by helium pycnometer (AccuPyc 1330, Micromeritics Instrument Corporation). The melt flow index (MFI) data were supplied by the manufacturers. The EEA copolymer is composed of 85 wt.% ethylene and 15 wt.% ethyl acrylate. The composition of the analyzed blend is 75 vol.% EEA and 25 vol.% PiBMA. The selection of this composition for the blend was based on the fact that greater amounts of PiBMA lead to stiffer blends, which are more suitable for the large dimensions co-extruded products. On the other hand, for thin co-extruded filaments, highly flexible compounds are desired, such that the filament can resist fracturing by stretching [22].

The glass transition temperature ( $T_g$ ) and the crystalline melting temperature ( $T_m$ ) of the pure thermoplastic materials were determined by differential scanning calorimetry (DSC; DSC 7, Perkin-Elmer). The analyses were carried out from 20 °C to 160 °C, with a heating rate of 20 °C/min, under a nitrogen atmosphere. The measurement procedure included heating the sample up to 160 °C, subsequently cooling it down to 20 °C and finally re-heating it up to 160 °C. The second heating curve is the one presented here because this is the most appropriate for interpretation, as the thermal history of the polymer is then known. The heat flow curves were normalized for the mass of the samples. Thermo-gravimetric analyses (TGA; TGA/SDTA 851<sup>e</sup> STAR<sup>e</sup> System thermo-balance, Mettler Toledo) were performed by heating the samples in an alumina crucible at 3 °C/min up to 600 °C. The TG scan was conducted in air to simulate the behavior of the sample under actual processing conditions.

The ceramic powder used was a commercially available lead zirconate titanate material (PZT/SKN-P505, CeramTec AG). When working with high solid loading ceramic-filled thermoplastic compounds, the degree of dispersion of the powder in the molten thermoplastic binder has a remarkable effect in obtaining homogeneous feedstocks and, as a result, defect-free

Table 1  
Selected information of the organic binders investigated.

Organic binder (Product – source)	Repeat unit	$M_w^a$ [g/mol]	Density [g/cm <sup>3</sup> ]	MFI <sup>b</sup> [g/10 min]
PS (Styron <sup>TM</sup> 648 – Dow Plastics)		104.15	1.05	1.3
PiBMA (Acryloid B67 – Lascaux)		142.20	1.04	<sup>c</sup>
LDPE (PEBD 1700MN 18C – Lacqtenne Elf Atochem S.A.)		28.05	0.92	70
EEA (Elvaloy <sup>®</sup> 2615 AC – DuPont <sup>TM</sup> )		128.17	0.93	6
Stearic Acid (93661, Fluka Chemie AG)	$H_3C-(CH_2)_{16}-COOH$	284.48	0.85	–

<sup>a</sup> Molecular weight of repeat unit.

<sup>b</sup> Melt flow index: 2.16 kg at 190 °C (ASTM D1238-ISO 1133).

<sup>c</sup> Value not supplied.

sintered bodies [23]. In view of that, the as-received PZT powder was initially coated with stearic acid (Table 1) as a surfactant. For this step, the appropriate amount of surfactant was firstly dissolved in toluene [20,23]. Afterwards, PZT powder was added and subsequently milled in a jar mill containing YSZ milling balls for 20 h. With the goal to ensure dispersion, the particle size distribution (PSD) of the as-received (uncoated) and of the coated powders was measured using a laser diffraction particle size analyzer (LS230, Beckman-Coulter Inc). Prior to the measurements, uncoated and coated PZT powders were dispersed in a toluene media and homogenized through ultrasonic treatment (HD 2070, Bandelin Sonopuls). The physical characteristics of the uncoated and the coated PZT powders are listed in Table 2. The specific surface area (SSA) was determined from a five-point  $N_2$  adsorption isotherm obtained from BET (Brunauer–Emmett–Teller) measurements (SA3100, Beckman-Coulter Inc). Referring to Table 2, a decrease in the PSD is observed in the presence of the stearic acid (coated PZT), emphasizing the effectiveness of the surfactant used.

A torque-rheometer (HAAKE PolyLab Rheomix 600, Thermo Fisher Scientific) was used to compound and record the rheological data of the as-received polymers (unfilled systems) and of the ceramic feedstocks (filled systems). After mixing the compositions at 10 rpm until the torque reached steady-state conditions, equilibrium torque values were recorded at rotor speeds ranging from 10 to 100 rpm with steps of 10 rpm at different temperatures. Table 3 describes the different systems analyzed, the mixing conditions and the temperatures used for the rheological characterizations. The equilibrium torque represented is the average value for the last 5 min of steady-state. The temperatures indicated in Table 3 are the temperatures measured inside the mixing chamber. A solid loading of 58 vol.% was selected for all the PZT-filled thermoplastic composites because it should provide a viscosity within a reasonable working range for the co-extrusion process [2] as well as a sufficient sintered density [24]. The stearic acid represents 7.7 vol.% of the ceramic feedstocks.

PZT green fibers were produced by extruding the different investigated feedstocks vertically through a die with a 300  $\mu\text{m}$  diameter orifice using a capillary rheometer (RH7 Flowmaster,

Table 2

Physical characteristics of the PZT/SKN powder.

PZT/SKN powder	Density [ $\text{g}/\text{cm}^3$ ]	SSA [ $\text{m}^2/\text{g}$ ]	PSD [ $\mu\text{m}$ ]
As-received (uncoated)	8.10	$1.97 \pm 0.01$	$d_{10} = 1.35$ $d_{50} = 2.66$ $d_{90} = 4.28$
Coated with stearic acid	7.25	$1.90 \pm 0.03$	$d_{10} = 0.57$ $d_{50} = 0.85$ $d_{90} = 2.07$

Rosand Precision Limited). The velocity of the piston was constant during the extrusion step ( $V_{\text{piston}} = 0.176 \text{ mm}/\text{min}$ ). The die swell ( $S_w$ ) of the extruded fibers was calculated as the ratio of the extrudate diameter to the orifice diameter of the die. The extrudate diameter was measured using an optical microscope (Wild M3Z, Leica) equipped with a micrometer (Mikrometer Mitutoyo 25 mm).

In order to produce PZT solid and hollow fibers by means of the co-extrusion process, a macro-preform composite formed by two different feedstocks was used. The primary feedstock contained the PZT-based ceramic which was to be micro-fabricated. The secondary one (fugitive feedstock) contained carbon-black as the fugitive material (BP<sup>®</sup> 120, Cabot Corporation, USA). The fugitive feedstock functions as space filler between the green filaments, provided that it can be completely removed after the micro-fabrication. For the solid-fiber production, in order to obtain the primary preform, the primary feedstock was extruded vertically through a 7.77 mm diameter die using the capillary rheometer mentioned before. The velocity of the piston was 5.0 mm/min at a defined temperature (temperature based on the characteristics of the thermoplastic binder used). To obtain the fugitive preform, the fugitive feedstock was uniaxially pressed (OPUS, Römheld) into a cylinder shaped feedrod (diameter = 24 mm, length = 45 mm). A hole with the same diameter of the primary preform was drilled in the center of the fugitive cylinder in order to structure the preform composites. The details of the co-extrusion process for solid-fiber production are described elsewhere [2]. The preform geometry for the hollow-fiber production was the opposite

Table 3

Mixing parameters and temperatures used for the rheological tests for the unfilled polymers and their feedstocks (58 vol.% PZT).

Systems	Mixing (at 10 rpm)			Rheological characterizations temperature, $T$ [ $^{\circ}\text{C}$ ]			
	Temperature [ $^{\circ}\text{C}$ ]	Maximum torque [Nm]	Equilibrium torque [Nm]	T1	T2	T3	T4
Unfilled PS	150	43.10	$15.89 \pm 0.20$	150	160	170	180
Unfilled LDPE	120	8.90	$3.30 \pm 0.01$	120	130	140	150
Unfilled EEA	120	17.14	$7.11 \pm 0.08$	120	130	140	150
Unfilled blend	120	17.00	$6.52 \pm 0.21$	120	130	140	150
PZT + PS	180	53.08	$11.00 \pm 0.43$	150	160	170	180
PZT + LDPE	120	20.04	$8.75 \pm 0.21$	120	130	140	150
PZT + EEA	120	37.24	$13.00 \pm 0.30$	120	130	140	150
PZT + blend	120	38.14	$13.31 \pm 0.14$	120	130	140	150

Note: PZT corresponds to PZT coated with stearic acid.

than the preform geometry for the solid-fiber production, i.e., the primary feedstock was uniaxially pressed into a cylinder-shaped feedrod (24 mm diameter), and the fugitive feedstock was extruded through a 7.77 mm diameter die. The preform composites were then structured drilling a hole in the center of the primary preform with the same diameter as the fugitive preform. The co-extrusions were carried out using the aforementioned capillary rheometer. The temperature was defined based on the characteristics of the thermoplastic binder material selected to prepare the feedstocks. A die with a half cone angle of 60°, 1 mm diameter and 16 mm length was used, so that the first extrudate was 24 times smaller than the initial preform (reduction ratio = 24:1). After binder and fugitive material removal and sintering of the ceramic (1100 °C, for 2 h), thin solid and hollow PZT fibers were attained. Scanning electron microscopy (TS5136MM, Tescan) was used to obtain cross-sectional micrographs from the fibers.

### 3. Results and discussion

#### 3.1. Unfilled thermoplastic binders: thermal behavior analyses

Fig. 2 represents the thermograms of unfilled thermoplastic binders, and Table 4 lists the information derived from these measurements. With reference to the amorphous polymers, the values of  $T_g$  indicated in Table 4 correspond to the averages between the onset and the final temperatures of the inflection from the baseline. Hence, the shift from the baseline verified between 106 and 115 °C for the PS, and the inflection between 52 and 70 °C for the PiBMA, correspond to the ranges of their  $T_g$ . For the LDPE and EEA copolymer, the peak temperature occurring at 107 and 104 °C is assigned to their  $T_m$ , respectively. The studied polymer blend (EEA + PiBMA) is determined to be compatible because the transition temperatures are slightly shifted when compared with the corresponding pure components. An incompatible blend would only show the characteristic DSC responses of the individual components [25]. The importance in determining the transition temperatures of the organic binders relies on the set-up of the processing temperatures. The mixing (feedstocks compounding) and the

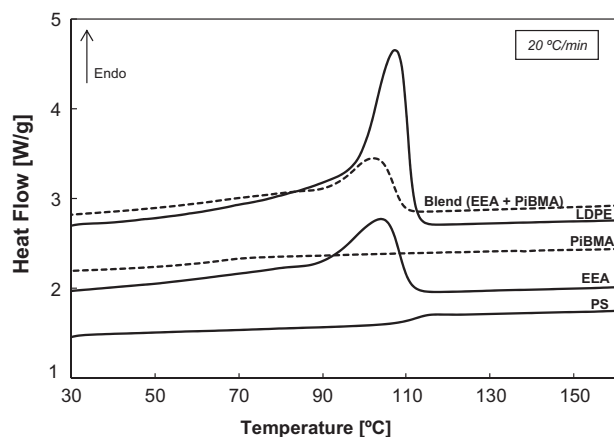


Fig. 2. DSC thermograms of the unfilled thermoplastic binders.

Table 4

Information derived from the DSC and TGA measurements of the organic binders.

Material	$T_m$ [°C]	$T_g$ [°C]	$T_{onset}$ [°C]	$T_{50}$ [°C]	$T_{max}$ [°C]
PS	Amorphous	111	260	315	315
PiBMA	Amorphous	61	226	269	271
LDPE	107	–	275	382	363
EEA	104	–	270	386	359
Blend	102	68	230	409	387
Stearic acid	62	–	150	215	223
Coated PZT	–	–	220	275	280

co-extrusion steps should be performed above the  $T_m$  and the  $T_g$  values for semi-crystalline and amorphous polymers, respectively, in order to facilitate the wetting of the powder.

The TGA of the organic systems is shown in Fig. 3. We derived from the TG curves the temperature at which weight loss onset occurs ( $T_{onset}$ ), the temperature that corresponds to the maximum decomposition rate ( $T_{max}$ ) and the temperature for 50% weight loss ( $T_{50}$ ), listed in Table 4. Additionally, Table 4 represents the parameters for the pure stearic acid and for the PZT powder coated with stearic acid. The parameters of the coated PZT were determined after normalizing the TGA results for the amount of stearic acid. Considerable differences in the thermal decomposition of the thermoplastic binders are observed in terms of both degradation temperature (Table 4) and pathway (Fig. 3). While the decomposition of the amorphous polymers (PiBMA and PS) occurs in a continuous stage, the semi-crystalline binders (EEA and LDPE) show distinct degradation steps. The addition of the amorphous PiBMA to the EEA polymer leads to a decreased  $T_{onset}$  of the blend when compared with the pure EEA; however,  $T_{50}$  and  $T_{max}$  increase. Additionally, as for the semi-crystalline binders, the blend shows distinct degradation steps. The amorphous binders present a lower final decomposition temperature than the semi-crystalline thermoplastics, which, depending on the sintering temperature of the ceramic used, would be of advantage.

The study of the thermal performance of the organic compounds stems from the need to correlate their degradation behavior to the processing steps. Processing (feedstocks compounding, preforms fabrication and co-extrusion) should be carried out at temperatures significantly below the binder  $T_{onset}$  to avoid drastic changes in the flow behavior of the feedstocks due to degradation of the thermoplastic material. For the case of the thermoplastic binders investigated within this study, the limiting temperature for processing is the  $T_{onset}$  of the coated PZT (lowest  $T_{onset}$  when compared with the thermoplastic binders, Table 4). The retention of the stearic acid during processing is necessary for the consistency of ceramic powder volume loading. In addition, if a degradation of the stearic acid during processing does occur, a change in the flow behavior of the composition might happen. It is noteworthy that the pure stearic acid starts decomposing at 150 °C, but an increase in 70 °C on the  $T_{onset}$  is measured when this molecule is adsorbed onto the particle surface of the PZT (Table 4). This is attributed to the strong physical bond between the stearic acid head group (COOH, Table 1) and the ceramic surface [23].



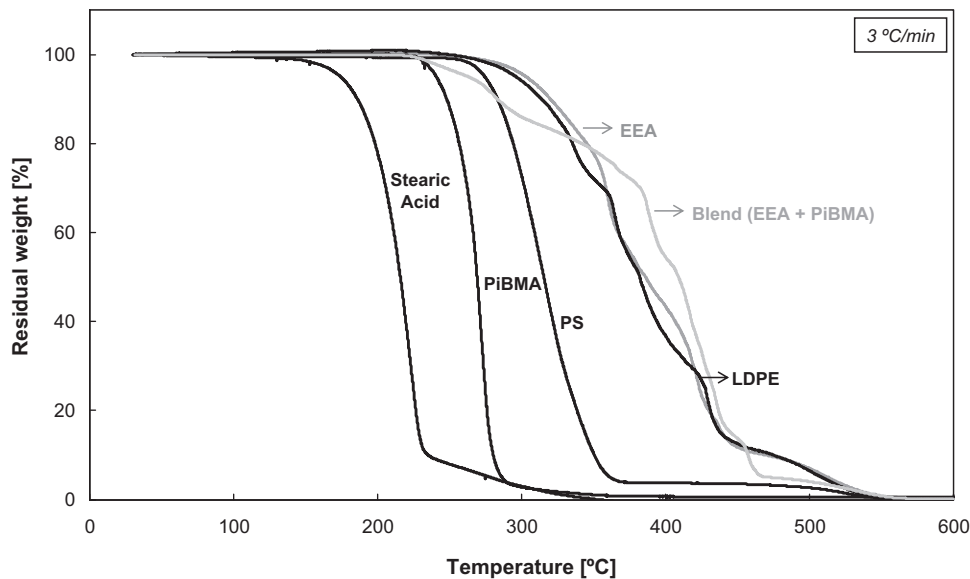


Fig. 3. Decomposition profiles of the unfilled organic binders.

TGA is additionally important in identifying temperature regions of rapid mass loss ( $T_{\max}$ ), which can be used as an initial guide in the set-up of the debinding process of the as-shaped ceramics. As previously discussed, the binder should be completely removed before sintering of the ceramic starts. It is verified that no residue was left for any of the investigated binders at 600 °C (Fig. 3), the temperature at which PZT starts sintering in case of PbO excess [26].

### 3.2. Unfilled and filled thermoplastic binders: rheology and processability

It is well known that the polymers provide the rheological properties required for ceramic feedstocks. However, the interactions between the thermoplastic binders and the ceramic particles also affect the flow behavior, and, as a result, the processability of the feedstocks is influenced. In this context, this section discusses the rheological behavior of the unfilled polymers in comparison with the corresponding filled mixtures.

Table 3 indicates the temperatures at which the mixing (feedstock compounding) and the rheological characterizations were carried out. The mixing and the first temperature for the rheological tests (T1) were set as low as possible to suppress thermal degradation of the organic materials ( $T_m$ ,  $T_g < T1 < T_{\text{onset}}$ ) and T4 was set to be lower than the  $T_{\text{onset}}$  of the thermoplastic binder ( $T4 < T_{\text{onset}}$ ). For the case of the filled systems, the  $T_{\text{onset}}$  of the surface-modified PZT (coated PZT) was the limiting working temperature (Table 4). For the polystyrene-containing systems, elevated temperatures ( $T1 \gg T_g$ ) were required due to the high torque values observed for the unfilled PS, an indicative of a highly viscous binder. Besides the equipment imposes a limit for maximum torque reading, high torque values may result in an elevated applied pressure during co-extrusion, fact that may lead to phase separation during extrusion. In addition, Table 3 gives the maximum and the equilibrium torque during the mixing step. Both parameters are dependent on the melt viscosity of the thermoplastic binder. It

can be seen that LDPE reveals the lowest viscosity (lowest torque), whereas PS shows the highest one (highest torque). The addition of PiBMA to the EEA co-polymer does not significantly influence its behavior. For the unfilled polymers, the maximum torque corresponds to the heat transfer necessary to completely melt the thermoplastic material. For the case of the filled polymers, the maximum torque value is indicative of the energy necessary to fill voids between particles and cover their surface.

Besides determining the aforementioned parameters during mixing, the torque-rheometer is, in addition, useful in providing information on the flow behavior of the materials. This can be attained when considering the torque-rheometer measuring head acting as two adjacent concentric-cylinder rheometers [27,28]. Neglecting end effects, the following equation is applied in concentric-cylinder rotational rheometers:

$$\eta_{app} = \frac{M}{\Omega} k \quad (1)$$

where  $\eta_{app}$  is the apparent viscosity,  $M$  the torque moment,  $\Omega$  the angular velocity and  $k$  is a constant that depends on the dimensions of the rheometer (internal and external radius,  $R_i$  and  $R_e$ , respectively, and cylinder length  $L$ ). A schematic representation of a torque- and a concentric-cylinder-rheometer and the corresponding analogy are given in Fig. 4. In view of this representation and considering Eq. (1), the torque moment ( $M$ ) can be related to the imposed shear stress ( $\tau$ ) and the rotor speed ( $N$ ) to the shear rate ( $\dot{\gamma}$ ):

$$\tau = k_1 M \quad (2)$$

$$\dot{\gamma} = k_2 N \quad (3)$$

therefore,

$$\eta_{app} = \frac{\tau}{\dot{\gamma}} = \frac{k_1 M}{k_2 N} \quad (4)$$

The melt viscosity of a polymer depends on the temperature used, which in turn has a pronounced effect on the processing

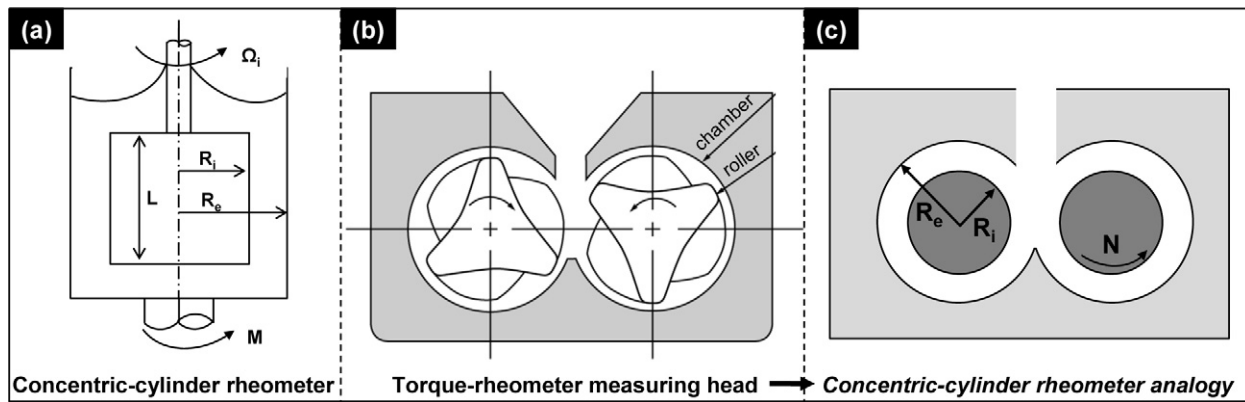


Fig. 4. Schematic representation of (a) concentric-cylinder and (b) torque-rheometers and, (c) the torque-rheometer analogy to a concentric-cylinder rheometer.

step. The temperature–viscosity relationship can be defined using an Arrhenius type equation [12]:

$$\eta_{app} = \frac{\tau}{\dot{\gamma}} = A e^{(E_f/RT)} \quad (5)$$

where  $\eta_{app}$  is the apparent viscosity at temperature  $T(K)$ ,  $A$  is the frequency term depending on the entropy of activation for flow,  $E_f$  is the energy of activation for viscous flow and  $R$  is the universal gas constant (8.314 J/mol K). Combining (4) with (5), derived from the rheological characterizations performed using torque-rheometry, Fig. 5 represents Arrhenius-type plots of

torque/rpm-temperature data for the unfilled polymers and their corresponding feedstocks.

Referring to Fig. 5, with respect to the temperature effect, all unfilled thermoplastic binders and feedstocks obeys an Arrhenius relation. Additionally, as expected, Fig. 5 points out that all measured systems exhibit pseudoplastic behavior for the temperature and shear ranges analyzed, as the apparent viscosity (torque/rpm) decreases with increasing shear rate (rpm). Filling the polymers increases the resistance to flow. The addition of ceramic particles to the system, besides decreasing the effective volume of polymer, leads to a reduction in the

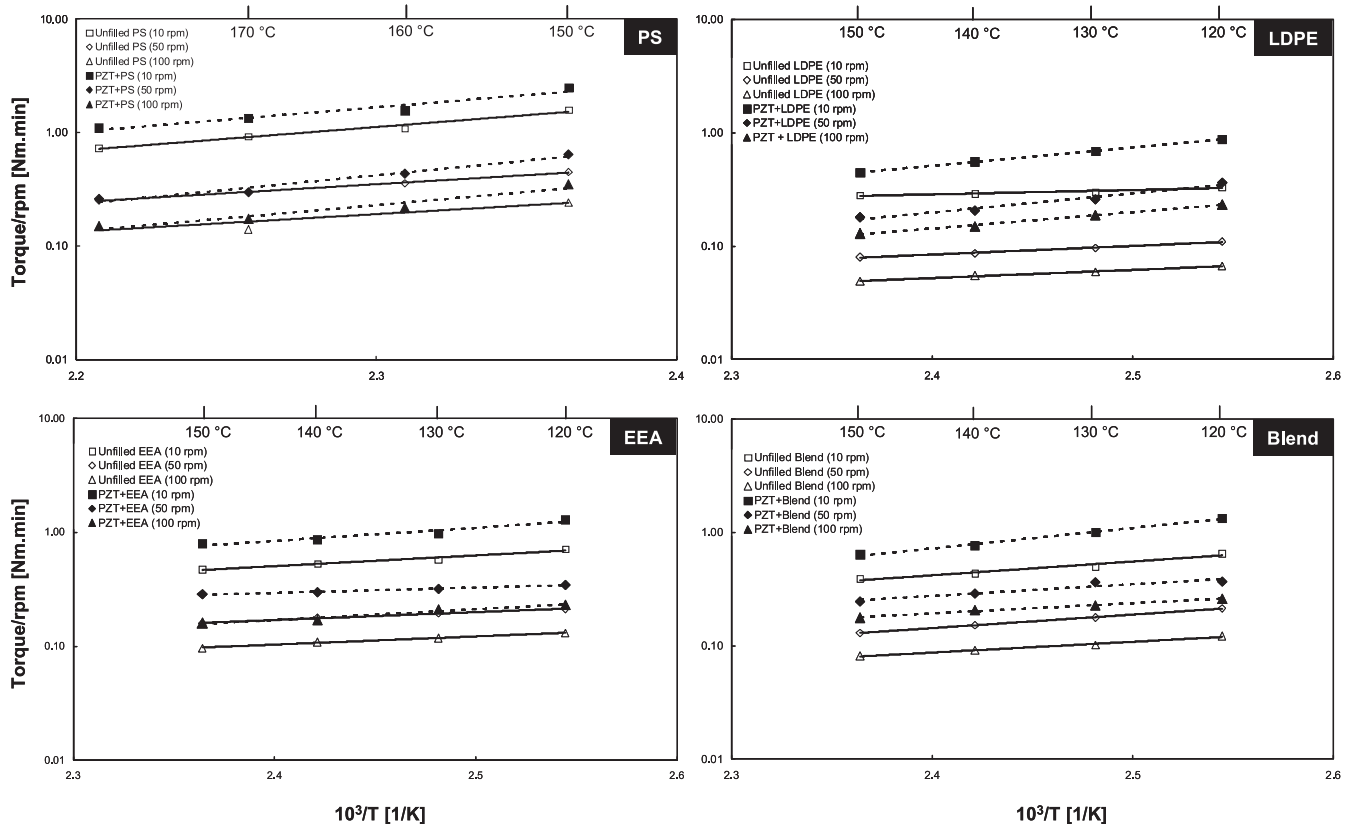


Fig. 5. Temperature dependence of viscosity (torque/rpm) for the unfilled polymers and their corresponding feedstocks (58 vol.% PZT). Note: temperature axes are different.

polymer chain mobility. The usefulness of Arrhenius representations is related to the potential correlation between the feedstock preparation and the co-extrusion steps: by determining the torque at a given temperature during compounding, the pressure necessary to co-extrude can be estimated. For example, in this study, equilibrium torque values down to 3 Nm at 10 rpm were an indication of very low viscous compositions, allowing the material to flow by gravity during the co-extrusion process when using a capillary die with 1-mm diameter. On the other hand, for feedstocks with equilibrium torque values higher than 30 Nm at 10 rpm, the pressure during co-extrusion through a 1-mm diameter die increased dramatically. The aforementioned correlation is of great importance for the co-extrusion technique, in which mixing and extrusion should be carried out at the same temperature [2], due to the sensitivity of viscosity to the temperature changes that polymers display. Accordingly, the Arrhenius representation is also functional in determining the accurate temperature in which different compositions can be co-extruded due to their similar viscosity.

Moreover, from Arrhenius plots it is feasible to determine the activation energy of viscous flow ( $E_f$ ), a measure of the resistance to flow of a given material. Fig. 6, derived from Fig. 5, shows the activation energy of viscous flow for the unfilled polymers and their corresponding feedstocks. The results found for the unfilled polymers (Fig. 6) are in good agreement with values for  $E_f$  previously reported in the literature [27,28]. When comparing the unfilled polymers with their corresponding feedstocks, an increase in  $E_f$  with the presence of the ceramic is observed for the PS and LDPE feedstocks, due to the fact that fillers lead to a decrease in the polymer chain mobility. However, for the case of the EEA and the blend, this assertion is not applicable. One possible explanation could be the presence of the ester functional group ( $-RCOOR'$ ) in the EEA and PiBMA binders (Table 1). This fact confers a polar character to the aforementioned binders, which would allow them to perform as dispersants, enabling a

better wetting of the inorganic filler. However, the compatibility of stearic acid (free and adsorbed) with polymer binder might also play an important role.

We consider that the energy barrier for viscous flow reflects the contributions of polymer–particle and particle–particle interactions. For all PZT feedstocks, the particle–particle interaction should be similar due to equal conditions of PZT powder and surfactant. Therefore, it is reasonable to correlate the  $E_f$  values of the feedstocks with the polymer–particle interaction; for a comprehensive comparison, the  $E_f$  values of the unfilled polymers should also be taken into account. Thus, referring to Fig. 6, a strong interaction of LDPE chains with PZT particles is assumed due to the abrupt change in the flow activation energy observed from the unfilled polymer and its feedstock. The PZT + PS compound also displays a high  $E_f$ ; however, so does the unfilled polystyrene. This can be explained by the low MFI of this binder (Table 1), what is an indicative of a high molecular weight polymer. The higher the molecular weight of a thermoplastic material, the greater the chain entanglements, which results in an increase in the melt viscosity, an occurrence that decreases processing ease. The feedstocks containing the EEA and the EEA blend do not show a strong polymer–particle interaction, as observed in the similar values of  $E_f$  for the unfilled polymers and their feedstocks (Fig. 6). During the ceramic–thermoplastic co-extrusion process, a strong polymer–particle interaction is desired in order to avoid phase separation. This phenomenon leads to an increase of the effective solid loading of the system, which results in modified flow properties. Taking into account the huge standard deviation verified for those aforementioned feedstocks (average  $E_f$  values for PZT + EEA =  $15.59 \pm 40\%$ ; average  $E_f$  values for PZT + blend =  $23.84 \pm 39\%$ ), it is reasonable to assume that at a particular shear rate (10, 50 and/or 100 rpm) the ceramic feedstock presented a lower  $E_f$  than its corresponding unfilled polymer. This lower  $E_f$  value might be attributed either to the presence of ester functional group in the EEA and PiBMA binders, as previously discussed; or to degradation of the thermoplastic binder, most likely occurred in the presence of the ceramic powder. It is important to mention that a change in color was observed after compounding those feedstocks, what is an indication of the degradation phenomena (results not shown). During mixing, high shear stresses in the particle-crowded condition may break the polymer into lower molecular weight fragments [29]. The decrease in the molecular weight of the binders decreases the activation energy of viscous flow.

Assuming that  $E_f$  reflects the contributions of polymer–particle and particle–particle interactions, the PZT + LDPE feedstock shows the strongest polymer–particle interaction. This might be mainly attributed due to its greatly branched chain structure, which increases the probability to form multi-adsorption sites on the ceramic particles.

### 3.3. Filled thermoplastic binders: extrusion and co-extrusion

After studying the rheology and processability of the unfilled and filled systems, the next logical step in the process was to extrude the filled thermoplastic binders to produce PZT fibers.

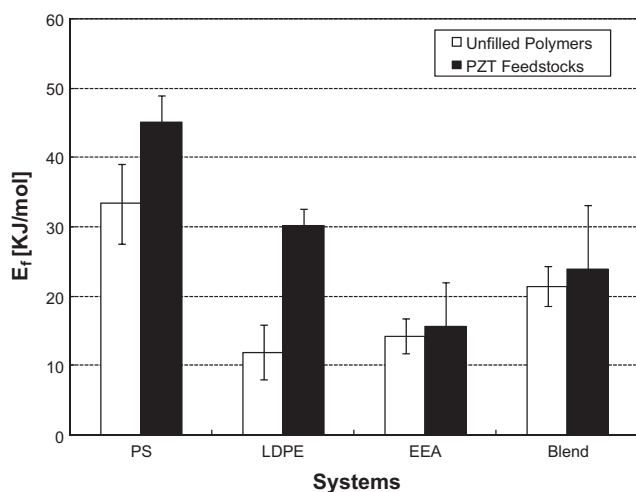


Fig. 6. Activation energy of viscous flow for the unfilled polymers and their corresponding feedstocks (58 vol.% PZT) at rotor speeds ranging from 10 to 100 rpm.



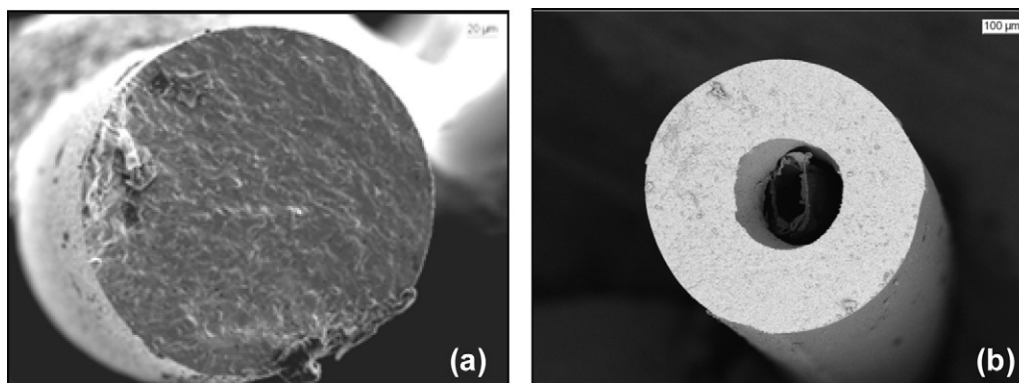


Fig. 7. SEM images of as-sintered (a) solid and (b) hollow PZT fibers obtained by the thermoplastic co-extrusion process using LDPE as the thermoplastic binder.

Due to the drawbacks of the polystyrene feedstock discussed to this point, such as its high apparent viscosity values (Fig. 5), this composition was not extruded. Table 5 points out the extrudate diameter and the die swell values for the PZT extruded fibers. It is observed that the PZT + LDPE feedstock presents the lowest  $S_w$  value, whereas the PZT + EEA shows the highest one. The addition of PiBMA to the EEA co-polymer (blend feedstock) decreases the  $S_w$  result of the EEA feedstock.

The die swell effect is an important parameter to be taken into account for composites shaped by co-extrusion. Besides the fact that feedstocks presenting high die swell may generate stress between the different co-extruded materials, this parameter is also essential for achieving final structures with geometries identical to the original preform.

In view of the results attained, based on the fact that the selection of the ideal binder for co-extrusion process requires consideration of parameters such as degradation during compounding of the feedstocks, the flow behavior as well as the final product dimension desired, the low-density polyethylene was selected within this work as the thermoplastic binder for the co-extrusion of thin PZT solid and hollow fibers. Under the investigated processing conditions, this binder exhibits low viscosity with a high solid loading, no indication of degradation, a strong particle–polymer interaction as well as a comparatively low die swell. Given that, successful co-extruded solid and hollow PZT fibers were obtained with the use of LDPE as the thermoplastic binder for both primary and fugitive feedstocks. Processing (feedstocks compounding, preform fabrication and co-extrusion) was carried out at 120 °C, temperature defined based on the results discussed for the LDPE binder. The debinding step was based on the TGAs of the feedstocks. Fig. 7 presents the cross-sectional micrographs of the sintered co-extruded solid ( $\sim 240$   $\mu\text{m}$  diameter) and hollow

( $\sim 800$   $\mu\text{m}$  diameter) PZT fibers. These ferroelectric fibers find their use as sensors and actuators.

#### 4. Conclusions

In this work, the essentials criteria to be considered for the selection of the proper thermoplastic binder for the formulation of ceramic co-extrusion feedstocks were presented. In order to ensure those discussed requisites, four pre-selected organic binders (polystyrene, low-density polyethylene, poly(ethylene-co-ethyl acrylate) and a blend of poly(ethylene-co-ethyl acrylate) and poly(isobutyl methacrylate)) were analyzed and their properties compared with lead zirconate titanate (PZT)-filled feedstocks. The analyses of the thermal behavior of the thermoplastic binders were fundamental in determining the optimum temperature range for processing (feedstocks compounding, preform fabrication and co-extrusion). The use of torque-rheometry to characterize both the unfilled and the filled thermoplastic binders was essential in verifying the thermal stability of the binders under processing conditions. With the use of an Arrhenius relation, the temperature dependency of viscosity could be determined and the energy of activation for viscous flow calculated. Arrhenius representation showed to be functional in estimating the co-extrusion behavior of the compounds at a given temperature. The flow activation energy results could retrospectively help to gain insight into the polymer–particle interactions.

Finally, the low-density polyethylene, due to its relatively low viscosity with a high solid loading, no indication of degradation, strong particle–polymer interaction as well as comparatively die swell, was used as the thermoplastic binder for efficiently producing thin solid (240  $\mu\text{m}$  diameter) and hollow (800  $\mu\text{m}$  diameter) PZT fibers by means of the co-extrusion technique. This research may function as the basis of further studies to select the optimal thermoplastic binder system to suit the processing conditions, which is indispensable information for successful co-extrusion.

#### Acknowledgements

We would like to thank Bohac WM and Bueno VL for helping with the experimental part and Martins CG and Koll B

Table 5

Extrudate diameter and die swell of the fibers extruded through a 300  $\mu\text{m}$  diameter capillary at 120 °C.

Feedstock (58 vol.% PZT)	Extrudate diameter [ $\mu\text{m}$ ]	Die swell $S_w$ [%]
PZT + LDPE	$321 \pm 5$	7
PZT + EEA	$359 \pm 6$	20
PZT + blend	$330 \pm 4$	10

Note: PZT corresponds to PZT coated with stearic acid.

for their comments. Additionally, we are grateful to CeramTec AG for supplying the PZT powder for this study.

## References

- [1] C. Van Hoy, A. Barda, M. Griffith, J.W. Halloran, Microfabrication of ceramics by co-extrusion, *J. Am. Ceram. Soc.* 1 (1998) 152–158.
- [2] M.R. Ismael, F. Clemens, W.M. Bohac, T. Graule, M.J. Hoffmann, Effects of rheology on the interface of Pb(Zr, Ti)O<sub>3</sub> monofilament composites obtained by co-extrusion, *J. Eur. Ceram. Soc.* 29 (2009) 3015–3021.
- [3] Z. Chen, K. Ikeda, T. Murakami, T. Takeda, Extrusion behavior of metal–ceramic composite pipes in multi-billet extrusion process, *J. Mater. Process. Technol.* 114 (2001) 154–160.
- [4] D. Kovar, B.H. King, R.W. Trice, J.W. Halloran, Fibrous monolithic ceramics, *J. Am. Ceram. Soc.* 80 (1997) 2471–2487.
- [5] A.F. Abouraddy, et al., Towards multimaterial multifunctional fibres that see, hear, sense and communicate, *Nat. Mater.* 6 (2007) 336–347.
- [6] S.M. Lee, S.H. Jun, C.S. Park, H.E. Kim, K.W. Lee, Spiral-shaped piezoelectric actuator fabricated using thermoplastic co-extrusion process, *Sens. Actuators A: Phys.* 148 (2008) 245–249.
- [7] S.M. Lee, C.S. Park, H.E. Kim, K.W. Lee, Helical-shaped piezoelectric motor using thermoplastic co-extrusion process, *Sens. Actuators A: Phys.* 158 (2010) 294–299.
- [8] M.J. Edirisinghe, J.R.G. Evans, Review: fabrication of engineering ceramics by injection molding. I. Materials selection, *Int. J. High Tech. Ceram.* 2 (1986) 1–31.
- [9] M. Wegmann, B. Gut, K. Berroth, Extrusion of polycrystalline ceramic fibers, *Ceram. Forum Int.* 75 (1998) 35–37.
- [10] F.J. Clemens, V. Wallquist, W. Buchser, M. Wegmann, T. Graule, Silicon carbide fiber-shaped microtools by extrusion and sintering SiC with and without carbon powder sintering additive, *Ceram. Int.* 33 (2007) 491–496.
- [11] J.A. Brydson, *Plastic Materials*, 7th ed., 1999.
- [12] A.V. Shenoy, *Rheology of Filled Polymer Systems*, Academic Publishers, Netherlands, 1999.
- [13] J.A. Lewis, Binder removal from ceramics, *Annu. Rev. Mater. Sci.* 27 (1997) 147–173.
- [14] J.S. Reed, *Principles of Ceramics Processing*, 2nd ed., John Wiley & Sons, Inc., New York, 1995.
- [15] A.M. Knapp, J.W. Halloran, Binder removal from ceramic-filled thermoplastic blends, *J. Am. Ceram. Soc.* 89 (2006) 2776–2781.
- [16] K.E. Hrdina, J.W. Halloran, Dimensional changes during binder removal in a mouldable ceramic system, *J. Mater. Sci.* 33 (1998) 2805–2815.
- [17] V.F. Janas, T.F. McNulty, F.R. Walker, R.P. Schaeffer, A. Safari, Processing of 1–3 piezoelectric ceramic/polymer composites, *J. Am. Ceram. Soc.* 78 (1995) 2425–2430.
- [18] A.A. Bent, N.W. Hagood, Piezoelectric fibre composites with interdigitated electrodes, *J. Int. Mater. Syst. Struct.* 8 (1997) 903–919.
- [19] C.E.A. Payne, J.R.G. Evans, Cross-flow ceramic structures produced by plastic processing, *Int. J. Adv. Manuf. Tech.* 14 (1998) 508–513.
- [20] J. Heiber, F. Clemens, T. Graule, D. Hülsenberg, Thermoplastic extrusion to highly-loaded thin green fibres containing Pb(Zr,Ti)O<sub>3</sub>, *Adv. Eng. Mater.* 7 (2005) 404–408.
- [21] J.F. Feller, D. Langevin, S. Marais, Influence of processing conditions on sensitivity of conductive polymer composites to organic solvent vapours, *Synth. Met.* 144 (2004) 81–88.
- [22] Y.H. Koh, J.W. Halloran, Green machining of a thermoplastic ceramic-ethylene ethyl acrylate/isobutyl methacrylate compound, *J. Am. Ceram. Soc.* 87 (2004) 1575–1577.
- [23] T.F. McNulty, D.J. Shanefield, S.C. Danforth, A. Safari, Dispersion of lead zirconate titanate for fused deposition of ceramics, *J. Am. Ceram. Soc.* 82 (1999) 1757–1760.
- [24] M.R. Ismael, F. Clemens, T. Graule, M.J. Hoffmann, Processing, microstructure and electromechanical properties of Pb(Zr, Ti)O<sub>3</sub> fibers obtained by thermoplastic co-extrusion, in: *IEEE International Symposium on the Application of Ferroelectrics*, 2009, doi:10.1109/ISAF.2009.5307603.
- [25] G.P. Simon, *Polymer Characterization Techniques and their Application to Blends*, American Chemical Society/Oxford University Press, Washington, D.C., 2003.
- [26] M. Hammer, M.J. Hoffmann, Sintering model for mixed-oxide derived lead zirconate titanate ceramics, *J. Am. Ceram. Soc.* 81 (1998) 3277–3284.
- [27] L.L. Blyler Jr., J.H. Daane, An analysis of Brabander torque rheometer data, *Polym. Eng. Sci.* 7 (1967) 178–181.
- [28] J.E. Goodrich, R.S. Porter, A rheological interpretation of torque-rheometer data, *Polym. Eng. Sci.* 7 (1967) 45–51.
- [29] J.F. Wight Jr., J.S. Reed, Polymer-plasticized ceramic extrusion, Part 1, *Am. Ceram. Soc. Bull.* 80 (2001) 31–35.